Discussion on relationship between fracture energy and fractured area of concrete-to-concrete surfaces

A. Satoh[1], K. Yamada[1], S. Ishiyama[1]
[1]*Akita Prefecture University, Yurihonjo, Japan*

1. Introduction

Every concrete structure has concrete-to-concrete surfaces as placing joints which are discontinuous planes in concrete produced during construction, which should inseparably adhere to each other for better performance. The adhesion of newly cast concrete with old concrete is the most critical issue for retrofitting existing concrete structure. The first issue to study for improving mechanical properties of interfacial adhesion performance in concrete is the thorough understanding of the mechanism of interfacial fracture. For that purpose, tension softening diagram (TSD) is the best resort. It means that TSD comprises the most fundamental features of fracture mechanics parameters [1] including tension softening initial stress (ft), critical crack width (Wcr) and fracture energy (GF).

In the recent studies [2, 3] about TSDs of specimens that have a placing joint, the authors pointed out that GF of placing joint is strongly related to the treatment applied to the surface of it. Also there was an interesting finding that tells GF was proportional to the fractured area which appeared on the surface of separated specimen [2, 3]. This paper succeeds the former study aiming at revealing an exact relationship between GF and the corresponding fractured surface. Then the authors predict GFs of placing joint from the GF of monolithic specimen to demonstrate that the contribution of fractured area to GF is the same, though the fractured area is not the same.

2. Experiment

2.1 Specimens for experiment

The authors prepared five types of concrete prisms, each of which has varied concrete-to-concrete joint surfaces made from different roughening or different form on them, and a type of monolithic specimens for the reference. The specimens' names are as follows; N for monolithic ones, J for ones cast with joint sheet [2], E for ones cast on a surface of exposed aggregate treated with retardant admixture, FS for ones cast on a fractured surface of concrete, R for ones roughened with steel wire blush and SP for ones with an as-cast surface on a form made of steel plate painted with fluoro-plastic. Table 1 shows mix proportion of concrete used for specimens, and Table 2 the attribute of specimens.

Table 1 Mix proportion of concrete

W/C	s/a	Weight of materials [kg/m^3]					Air	slump
[%]	[%]	Water	Cement	Sand	Gravel	Ad	[%]	[cm]
51.4	43.0	177	344	739	1010	1.72	3.0	22

Ad: Super Plasticizer

The number of specimens was three for each case, which have a section of 100 mm by 100 mm and a length of 400mm. The joint specimens were made through two times of casting, which was treated after first casting and second concrete was cast afterwards. In the case of R, before second cast of concrete, the joint surface was roughened with a wire brush. Then concrete was cast in the opposite half of the mold as depicted in Fig.1. The specimens were cured in water at 20 $^{\circ}C$ for 28 days after the second cast of concrete. A 50 mm depth notch was incised at the center of the specimen before fracture mechanics test.

Table 2 Attributes of specimens

Specimen	Surface condition	Elapsed time after 1st cast
N	(Monolithic)	-
J	Joint sheet	24hours
E	Exposed aggregate	24hours
FS	Fractured surface	35days
R	Roughened with steel wire brush	24hours
SP	As cast	24hours

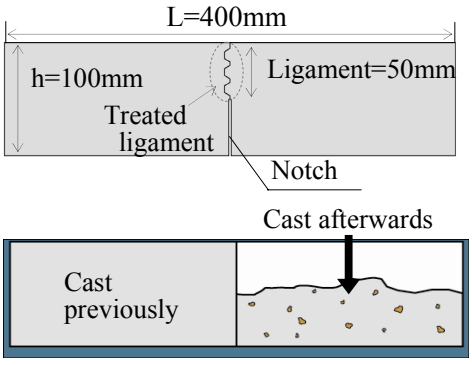

Fig. 1 Detail of specimen (above) and method for producing specimen (below)

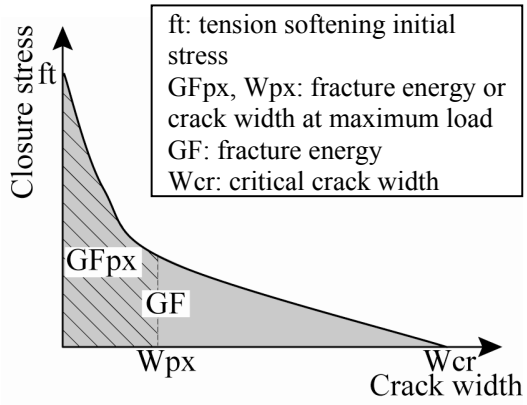

Fig. 2 Typical TSD

2.2 Fracture mechanics test and inverse analysis

The authors conducted a series of fracture mechanics test with observing RILEM's recommendation [4]. Load and crack mouth opening displacement (CMOD) were measured continuously during the loading. To cancel the dead weight of specimen, and to obtain a precise measurement, a counter weight made of steel was glued at both ends of specimens. Servo type loading machine was used to get high-speed response with the help of feed-back system in the machine.

TSD was achieved from the load-CMOD curve of specimen with employing multi-linear approximation method which was standardized by JCI [5]. Fracture energy is consumed energy during the fracture of a ligament of a specimen, which can be displayed as an area enclosed with x-axis, y-axis and TSD in the graph.

Fracture energy consumed until the maximum load in fracture toughness test is abbreviated to GFpx in this study. In Fig. 2, ft is tension softening initial stress which has the same meaning of tensile strength evaluated by the fracture toughness test. Wpx is the crack width when load reaches the maximum value in the test and Wcr is the crack width when load becomes zero (critical crack width).

2.3 Observation of fractured surfaces

After fracture mechanics test, the ligaments of separated specimens were sliced for the careful observation to distinguish fractured part from smooth part. The smooth part looked whitish and looked as if the surface detached without any resistance.

The fractured part had a rough surface where some fine aggregates or a lump of CSH gel were observed measuring above about 0.2mm or more. The authors should have used 3-dimensional laser ray positioning machine for measuring the precise shape of the ligament of specimen FS because the old surface to be cast afterwards was a fractured rough surface in this specimen. The fractured part was distinguished with the help of image analyzer in this case. Then finally, the sliced samples were incised again to small pieces for the observation with scanning electron microscope (SEM).

3. Results

3.1 Mechanical performance of joint

Table 3 shows the fracture mechanics parameters. The authors calculated flexural strength (fb) in the Table for only the reference of strength, though the value does not have a real meaning of surface stress. The resulted GFs are ranging from 0.01N/mm (specimen SP) to 0.05N/mm (specimen J) indicating they are small compared to the reference value of 0.1N/mm for specimen N.

The joint with roughened surfaces such as specimen J, R and E have good results among joints tested here. But the joint cast on a very rough surface of a fractured ligament (specimen FS) did not produce good results. One of the reasons for it would be due to the elapsed time after second casting (35 days) for specimen FS that decreases unhydrated cement on the surface of joint. Another reason would be the emergence of coarse aggregates which would produce a weak transient layer of calcium hydroxide on the surface.

There are some important remarks to be mentioned regarding Table 3. The ratio of GF from strongest joint divided by that from weakest joint reaches about 5, indicating the adequate roughening is very essential for the enhanced mechanical performance of the joint. The interesting finding is that the ratios of fb or ft divided by the ones of weakest joint are about 2 to 3, which are far smaller than the ones of GF. This result is the same as the one from a previous research by Kurihara [6].

Table 3 Fracture mechanics parameters

	fb [Mpa]	ft [Mpa]	Wcr [mm]	W_{Px} [mm]	GF [N/mm]	GF_{Px} [N/mm]
N1	4.94	6.82	0.213	0.011	0.0911	0.0296
N2	4.85	7.07	0.130	0.007	0.0955	0.0261
N3	4.60	7.28	0.224	0.013	0.1160	0.0299
J1	3.74	5.80	0.200	0.007	0.0597	0.0160
J2	3.80	5.56	0.051	0.007	0.0467	0.0169
J3	3.53	4.76	0.117	0.010	0.0501	0.0188
E1	2.85	2.90	0.113	0.007	0.0340	0.0104
E2	3.12	3.92	0.049	0.006	0.0343	0.0119
E3	2.80	3.26	0.083	0.008	0.0372	0.0119
FS1	1.61	2.11	0.094	0.006	0.0243	0.0044
FS2	2.01	2.90	0.088	0.005	0.0211	0.0056
FS3	2.11	2.11	0.105	0.007	0.0288	0.0074
R1	3.42	6.47	0.047	0.003	0.0407	0.0107
R2	3.03	5.68	0.054	0.005	0.0297	0.0101
R3	3.60	5.52	0.038	0.007	0.0336	0.0140
SP1	2.00	3.65	0.028	0.003	0.0112	0.0039
SP2	2.20	3.49	0.027	0.003	0.0129	0.0045
SP3	1.75	3.03	0.071	0.006	0.0131	0.0047

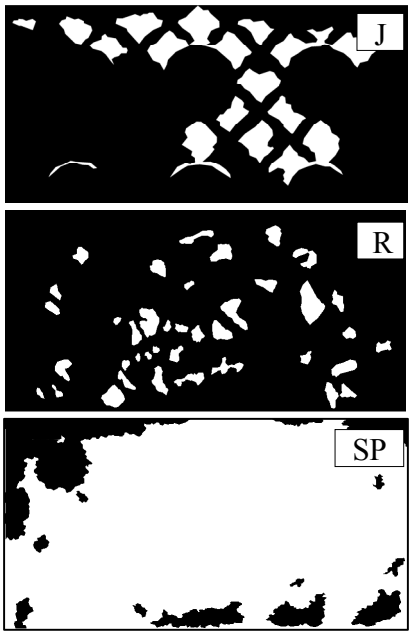

Fig. 3 Map of fractured surfaces
(black: fractured, white: detached)

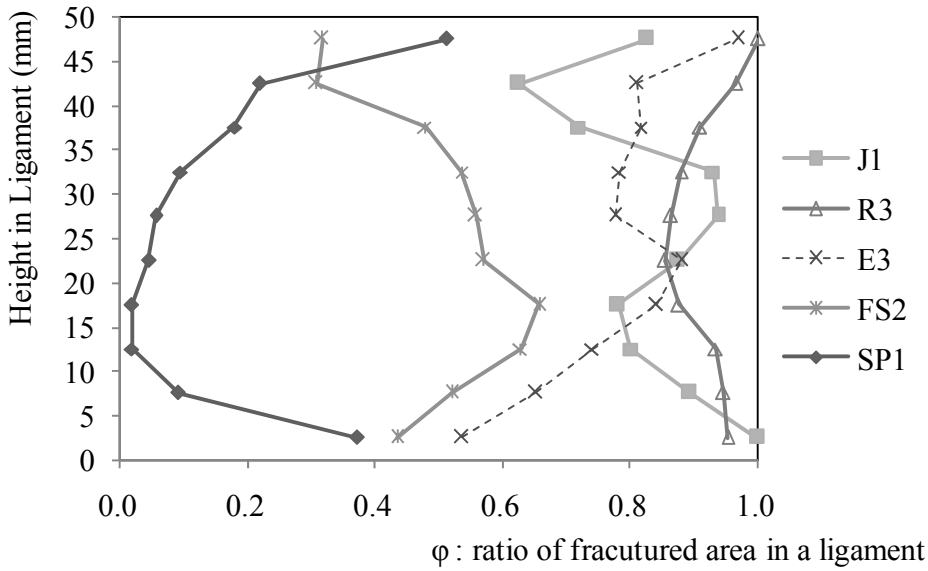

Fig. 4 Ratio of fractured area as a function of height in ligament

3.2 Observation of fractured ligament

The authors classified the surface of fractured ligament in two types after fracture mechanics test. One is a fractured part and the other is a detached part. On the basis of eye estimation, the authors refer to whitish and smooth areas as the detached part, and refer to exposed aggregates or rough part as the fractured part. Fig. 3 shows maps of fractured surfaces of specimen J, R and SP, in which the fractured part was depicted in black color while the detached part in white color.

In Fig.4, y-axis represents height in ligament and x-axis the ratio of fractured area divided by total area of ligament from the results of Fig.3. The ratio is expressed as φ in this paper. The distribution of φ is different from each other influenced by the conditions of treatment of the joint. There is a strong tendency that the larger the φ becomes, the better the mechanical properties of adhesion between concrete-to-concrete surfaces, as the authors remarked in the previous studies [2, 3].

4. Discussion

4.1 Fracture energy consumed in ligament

The authors used the same method as modified J-integral method [7] for the prediction of GF of a joint based on the total energy consumed in the ligament (not base on TSD or work of fracture). The well known modified J-integral method assumes the crack width to have a linear distribution as shown in Fig.5. At first, GF is expressed by Eq.(1) as an integral of TSD with respect to crack width (w). The entire fracture energy consumed in the ligament should be summed up from the bottom to the top of the ligament, which amounts to be E(w) in Eq.(2) [7].

$$GF(w) = \int_0^w \sigma(w)\,dw \tag{1}$$

$$E(w) = \int_0^{a_0} \left\{ \int_0^w \sigma(w)\,dw \right\} dA \tag{2}$$

In Eq.(1), $\sigma(w)$ is closure stress and w is crack width shown in Fig.5. In Eq.(2), E(w) is fracture energy consumed with total area of ligament, a_0 is the total length of propagated crack, A is area of fractured part.

4.2 Calculation of GF for joint specimen

The following equations were drawn for calculating GF of specimen X referring to Fig.5 and Fig.6. Fig.5(a) shows a crack width distribution of specimen N and Fig.5(b) the joint specimen X. Both of them reached respective critical crack widths; $Wcr_{(N)}$ for specimen N and $Wcr_{(x)}$ for specimen X. Because $Wcr_{(x)}$ is smaller than $Wcr_{(N)}$, the location where the width is $Wcr_{(x)}$ is above the bottom as shown in Fig.5(a). The $GF(Wcr_{(X)})$ for GF of specimen X and $GF(Wcr_{(N)})$ for GF of specimen N are expressed in Fig.6.

The authors adapted following assumptions.

(1) Only the area in fractured part contributes to GF, and the area in detached part does not.
(2) The fracture energy used for breaking the fractured part of ligament is the same regardless of the joint type in specimen. In other words, closure stress of fractured area is the same, though the fractured total area is different.
(3) The crack width distribution is linear retaining the same crack opening angle θ during crack propagation as shown in Fig.5(b).

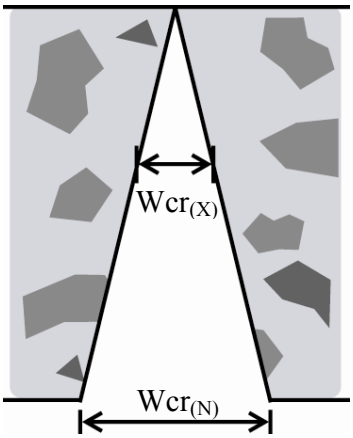

(a) Reference specimen N

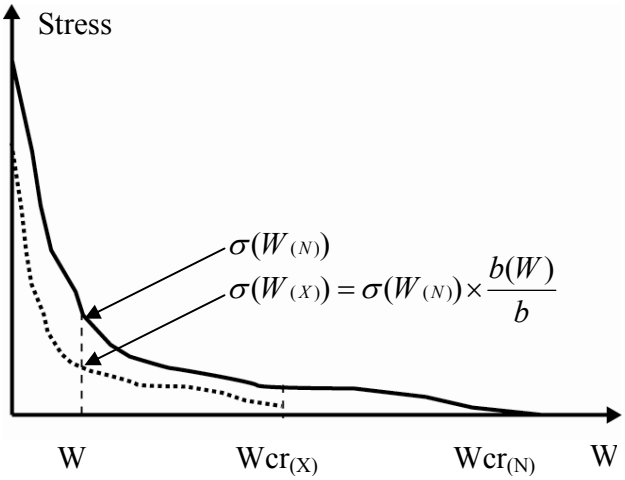

(a) TSD of specimen X and specimen N

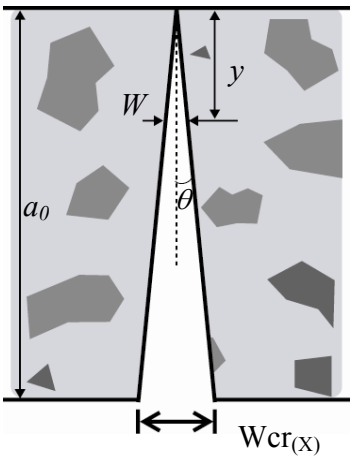

(b) Joint specimen X

Fig. 5 Crack width distribution

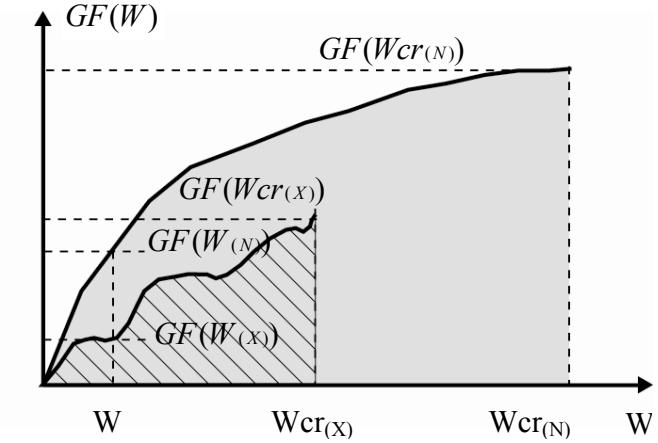

(b) GF(w) of specimen X and specimen N

Fig. 6 TSD and corresponding GF(w)

The advance of crack height (dy) and crack width propagation (dw) have a linear geometric relation referring to Fig.5(b) and to the assumption (3), i.e.,

$$\frac{dy}{a_0} = \frac{dw}{Wcr_{(X)}} \tag{3}$$

The assumption (2) leads to the following expression of closure stress as depicted in Fig.6(a), where b is total width of specimen (100mm) and b(w) is the width of fractured part at the given crack width W.

$$\sigma(W_{(X)}) = \sigma(W_{(N)}) \bullet \frac{b(W)}{b} \tag{4}$$

The Eq.(2) is rewritten using $Wcr_{(X)}$ instead of w for the specimen X.

$$E\left(Wcr_{(X)}\right)=\int_0^{a_0}\left\{\int_0^{Wcr(X)}\sigma\left(W_{(X)}\right)dw\right\}dA \tag{5}$$

The area dA is rewritten using Eq.(3) and considering that $Wcr_{(X)}=2a_0\tan\theta$, where θ is crack opening angle.

$$dA=b\bullet dy=b\bullet a_0\bullet\frac{dw}{Wcr_{(X)}}=\frac{b\bullet dw}{2\tan\theta} \tag{6}$$

When Eq.(4) and Eq.(6) are used in Eq.(5), the final expression of consumed fracture energy is achieved as Eq.(7). The Eq.(7) allows us to predict the fracture energy of joint specimen X from closure stress of monolithic specimen N.

$$E\left(Wcr_{(X)}\right)=\frac{1}{2\tan\theta}\int_0^{Wcr(X)}\left\{\int_0^{Wcr(X)}\sigma\left(Wcr_{(N)}\right)dw\right\}b\left(w\right)\bullet dw \tag{7}$$

GF is consumed energy per unit area, then the total fracture energy $E\left(Wcr_{(X)}\right)$ in Eq.(7) should be divided by Alig for getting $GF\left(Wcr_{(X)}\right)$. Where Alig is total area in the ligament.

$$GF\left(Wcr_{(X)}\right)=\frac{E\left(Wcr_{(X)}\right)}{Alig} \tag{8}$$

Fig.6(b) tells that $GF\left(Wcr_{(X)}\right)$ is reduced energy in terms of crack width and b(w). It means that critical crack width is reduced from $Wcr_{(N)}$ to $Wcr_{(X)}$. Also b(w) for specimen X is a reduced width from the width of specimen N which is full width of the specimen (100mm).

4.3 Calculation of GFpx for joint specimens

In the previous study [3], the authors proposed a stress distribution model by which moment at the section can be calculated. Fig.(7) is the resulted model. The previous study [3] also showed that crack opening angle θ is peculiar to the joint type in specimen and it retains the same value when the crack tip progresses heading for the top of the ligament. Fig.(8) is the resulted graph, which tells that crack opening angle θ is strongly related to ft.

When ft is known from TSD, then one can know the crack opening angle θ from Fig.(8). Inverse analysis of TSD tells the crack width (Wpx) at the maximum load in fracture toughness test. Then the height of crack tip (αx) is known with dividing Wpx by $2\tan\theta$. After these values were known, GF at the maximum load (GFpx) is calculated in the same way.

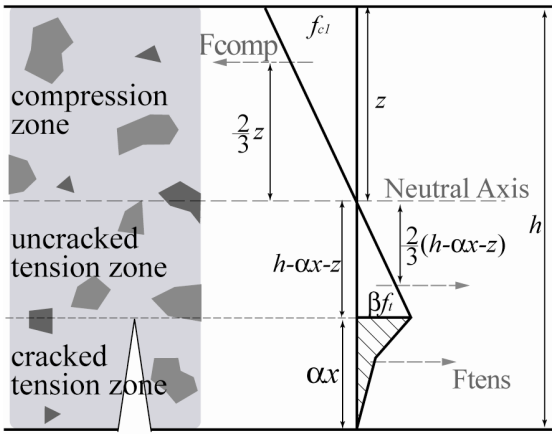

Fig.7 Stress distribution model [3]

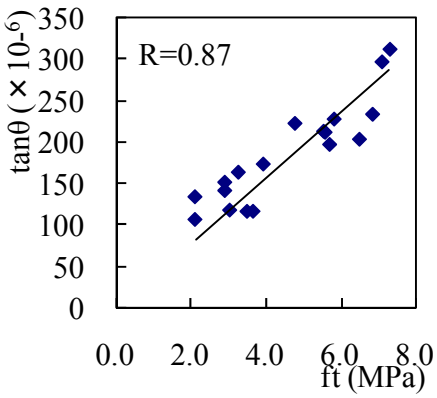

Fig.8 Relationship between crack opening angle and ft

4.4 Consistency of the proposed method

A comparison between experimental GF and the ones predicted by the proposed method is depicted in Fig.9 for GF and Fig.10 for GFpx. Both predicted GF and GFpx have good agreement with experimental ones indicating 0.86 and 0.78 as a correlation coefficient respectively.

With respect to the prediction of GFpx, the predicted values tend to be slightly lower than the experimental ones. One possible reason for that would be the insufficient prediction method of the crack tip height, which may predict a smaller area (αx × specimen width) than the real one.

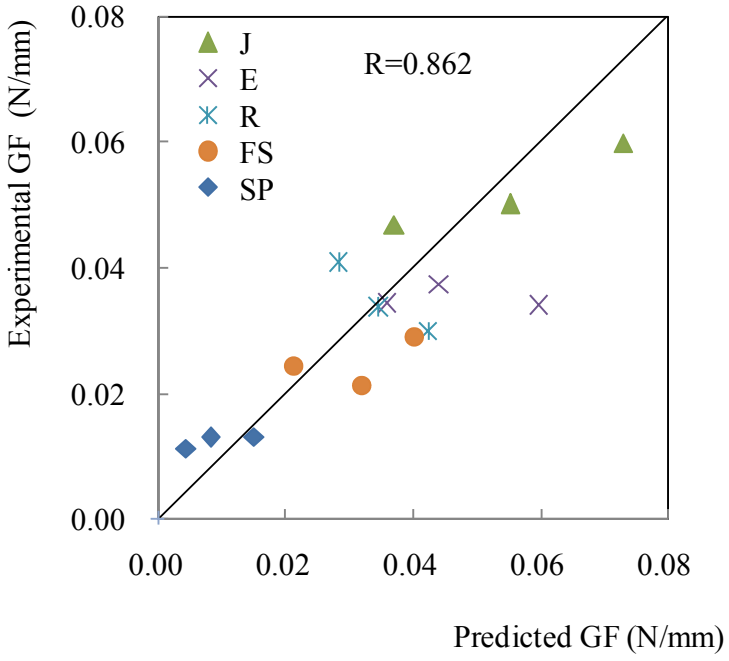

Fig. 9 Relationship between predicted and experimental GF

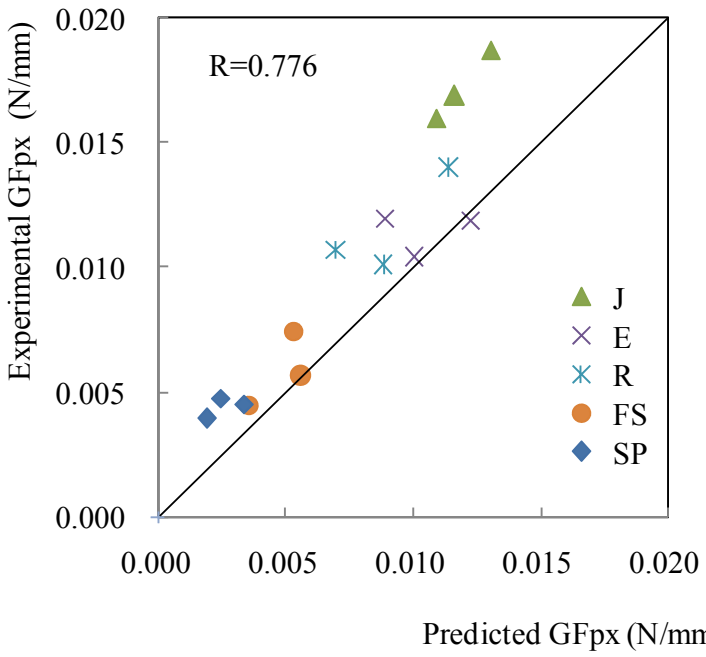

Fig.10 Relationship between predicted and experimental GFpx

4.5 Relationship between fracture energy and fractured area

The consistency of the predicted and experimental GF tells the validity of the assumptions (1) through (3). The most interesting issue is the assumption (2), which presumes the closure stress of fractured part is the same regardless of the joint type as long as the area is fractured. This means that the TSD of joint specimen is the reduced TSD of monolithic one in terms of the detached area of specimen, as is depicted in Fig.6(a).

The authors observed fractured part and detached part of all the surfaces of specimens with SEM. Fig.11(a) shows SEM photo of specimen SP where smooth layer is observed, which is characterized as $Ca(OH)_2$. This layer is so weak that it can not bear the closure stress. On the other hand, fractured surface of specimen R resembles the surface of specimen N (Fig.11(c)). This is the main reason that the fractured part has the same contribution to closure stress.

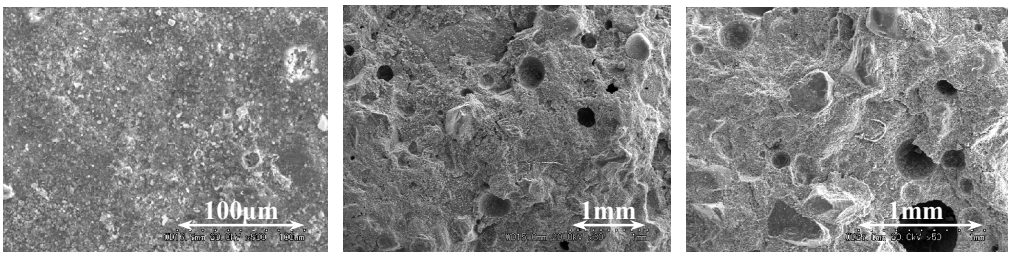

(a) Specimen SP (b) Specimen R (c) Specimen N

Fig.11 SEM photos from separated ligaments

5. Conclusions

The authors conducted fracture mechanics test of six types of concrete prism which have different concrete-to-concrete surfaces. After fracture toughness test, the ligaments were carefully observed to distinguish between fractured part and detached part. Tension softening diagrams of them were obtained, which were used to predict GF of joint specimen. With using them the authors discussed the relationship between GF and the area of the fractured part.

The findings are as follows.

[1] Contribution of the fractured part in the ligament of joint specimen to the closure stress is considered to be nearly the same as the fractured part in the ligament of monolithic specimen when judged with GF.

[2] The assumptions used to predict GF was reasonable; linear crack width distribution retaining the same crack opening angle θ, the relation between ft and θ as well as stress distribution model in the ligament were verified.

[3] SEM observation revealed that the appearance of fractured part in joint specimen resembles that of the monolithic specimen.

References

[1] H. Mihashi, Survey of Fracture Mechanics of Concrete, Concrete Journal, 25(2) (1987) 14-25

[2] K. Yamada, A. Satoh, S. Ishiyama, Evaluation of adhesion characteristics of joint in concrete by tension softening properties, Proceedings of "Fracture Mechanics of Concrete and Concrete Structure" , 3 (2007)1753-1759

[3] A. Satoh, K. Yamada and S. Ishiyama, A Discussion on Fracture Energy of Vertical Joint in Concrete, Proceedings of 17th European Conference on Fracture (ECF at Brno) (2008) 1530-1537

[4] RILEM Draft Recommendation, Determination of the Fracture Energy of Mortar and Concrete by Means of Three-point bend Tests on Notched Beams, Materials and Structures, 18(106) (1985)285-290

[5] JCI, Izumi, I. (eds), Test method for fracture energy of plain concrete (Draft) in JCI standards, JCI, Tokyo (2004)

[6] T. Kurihara, T. Ando, Y. Uchida and K. Rokugo, Evaluation of adhesive performance of construction joint in concrete by tension softening diagram, Proceedings of annual meeting of JCI, 18(2) (1996)461-466

[7] Y. Uchida, K. Rokugo and W. Koyanagi, Measurement and prediction of tension softening diagram based on bending test, Journal of JSCE, V-14(426) (1991)203-212